DX.DOI.ORG//10.19199/2022.165.1121-9041.022

Considerations on the Glide Snow Avalanches based on the Stauchwall *Model*

Nicola Viale*
Barbara Frigo*
Giulio Ventura*

* Polytechnic of Turin; Department of Structural, Geotechnical and Building Engineering. Turin, Italy.

Corresponding author:
nicola.viale@polito.it

Avalanches are natural events that can have consequences such as silvicultural losses, infrastructural damages, fatalities. In this paper, the attention is given to glide avalanches starting by a glide crack, a tensile crack that propagates at the crown – the upper release limit – due to the internal stress variation. However, the presence of a glide crack does not always give rise to a glide avalanche. In fact, when the slab starts to move, interacts with the stauchwall (the downslope boundary of the slab) which can fail or withstand.The Stauchwall model was adopted in order to verify if the gliding avalanche is triggered or not, by analyzing the dynamic stability of a slab subjected to an initial perturbation. In this paper, the model has been expanded by coupling it with a stress failure criterion.Thanks to this new failure criterion, it is possible to investigate the possible causes of subsequent glide avalanches triggering (in terms of hours or even days) after the crack propagation. In addition, the effect of a skier's fall/brake on the slab stability is analyzed. Finally, a sensitivity analysis of the model pointed out the important role played by the basal snow/soil friction.Therefore, it is shown that actions meant to increase this characteristic may be taken into account to effectively prevent glide avalanches.

Keywords: Glide avalanches, Stauchwall model, Full-depth avalanches, Avalanche release, Shear strength, skier.

1. Introduction

Snow avalanches are natural phenomena that can cause transportation problems, damages to structure and infrastructures, fatalities, etc. Usually, avalanches can be categorized as dry or wet snow avalanches (Peitzsch *et al*. 2012). Wet avalanches still represent a fascinating topic since it is difficult to forecast and control/trigger them using explosives (Baggi and Schweizer 2009; Peitzsch *et al*. 2012; Stimberis and Rubin 2011; Simenhois and Birkeland 2010; Lackinger 1987).

In this work, the attention is given to snow glide avalanches which can be considered as wet avalanches (McClung and Schaerer 1993). The snow gliding is a translational motion of a whole snow slab due to gravitational forces (der Gand and Zupančič 1965; McClung 1981). This motion is more probable to happen when the ground surface has reduced basal friction (e.g. grassy or smooth rocks), the slope inclination is higher than 15°, the snow-ground interface has a temperature of 0°C and/or liquid water is present in this interface, etc... (Conway and Raymond 1993; der Gand and Zupančič 1965; Lackinger 1987; McClung 1981; McClung and Clarke 1987). It is possible that a crack propagates at the upper limit of the slab due to the development of tensile stress generated by the snow gliding (Feistl *et al*. 2013). This crack is named glide crack and has a typical half-moon shape. This propagation coincides with a change of the slab equilibrium (Fig. 1). Therefore, the slab starts to move downwards and a force redistribution takes place from the crown to the stauchwall (Bartelt *et al*. 2012a; Ancey and Bain 2015). If the stauchwall is able to withstand the force redistribution, a new equilibrium of the slab is obtained; otherwise the glide avalanche is triggered (Bartelt *et al*. 2012a; Feistl *et al*. 2013). It seems clear that there are only two possible situations after the crack opening: (i) an immediate avalanche release, or (ii) the new equilibrium is preserved. However, delayed releases may happen. In these cases, the delay between the crack propagation and the glide avalanche release can range from hours to weeks (Ancey and Bain 2015).

Bartelt *et al*. 2012a presented a model – the Stauchwall model – meant to study the slab-stauchwall interaction after the crack propagation (Fig. 1). Here, the slab is assumed as a rigid body and the stauchwall as an homogeneous and viscoelastic one. After the crack propagation, in the transient state, the stauchwall may reach the critical strain rate $\dot{\varepsilon}_{cr}$ which implies its failure and the avalanche release. Otherwise, it is considered that the stauchwall does not fail and that the slab reaches a new equilibrium.

In the present paper, the Stauchwall model is coupled with a stress failure criterion in order to also consider the possibility that a snow glide avalanche release is due to the achievement of the shear strength τ_{cr} of the stauchwall. This new model is named Stuachwall stress model. Thanks to this new failure criterion, it is possible to examine the causes of delayed releases and define operative methods meant to trigger instable slabs on the slope after the crack propagation.

In addition, the skier's fall/bra-

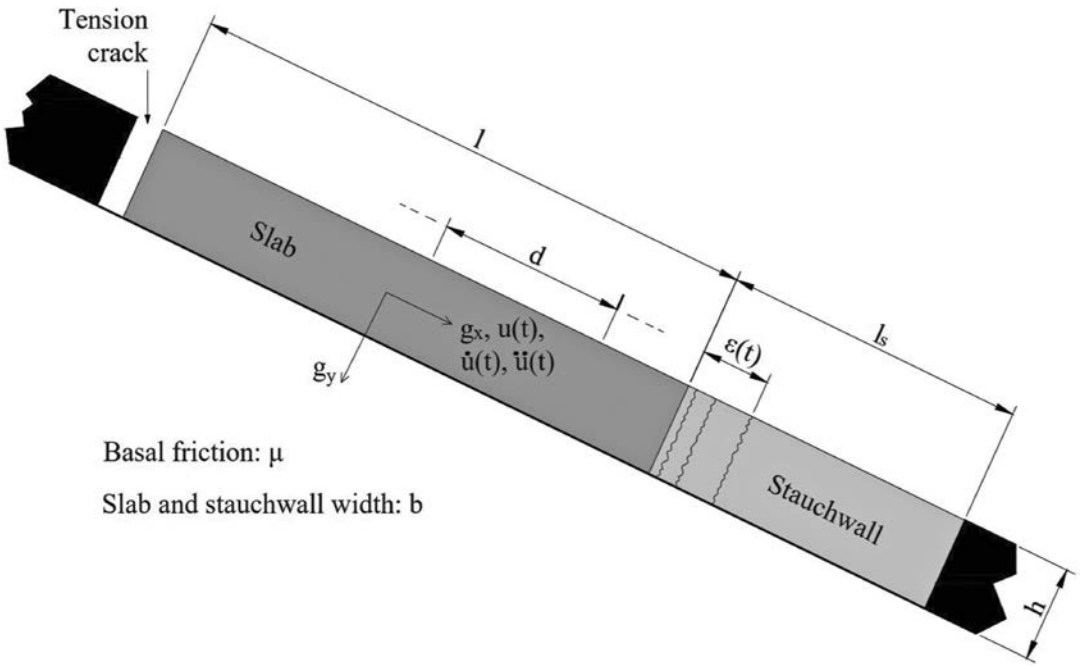

Fig. 1 – Schematic representation of the snowpack after the crack propagation. g_x and g_y are the components of the gravity acceleration parallel (g_x) and perpendicular (g_y) to the slope. $u(t)$, $\dot{u}(t)$, and $\ddot{u}(t)$ are, respectively, the displacement, velocity, and acceleration of the slab. The strain at the stauchwall is denoted by $\varepsilon(t)$. d is a generic distance on the slab which it is assumed that an eventual skier falls/brakes and stops his motion.

ke effects on the slab-stauchwall stability are investigated and a sensitivity analysis is performed in order to point out the parameters that have the largest influence in the model results. The same analysis is then used to demonstrate how small increases of basal friction may be used to prevent snow glide avalanches.

1.1. The Stauchwall model

As introduced, the Stauchwall model (Bartelt *et al*. 2012a) is adopted in the present work. Several applications and discussions regarding this model are present in literature (e.g. Bartelt *et al*. 2012a; Feistl *et al*. 2013; Feistl *et al*. 2014; Höller 2014; Ancey and Bain 2015). A small summary regarding this model is presented in the following paragraphs.

The Stauchwall model assumes that a prismatic monolithic slab (having density ρ, length l, depth h, and width b) starts to move on a slope inclined of ψ at the time t = 0 to which corresponds the crack formation. It is hypothesized the presence of a basal friction μ under the slab. It has to be $\mu < \tan\psi$ in order to let the slab start the motion. Due to the slab movement ($t \geq 0$), the stauchwall undergoes to an axial strain $\varepsilon(t)$ and to an axial stress $\sigma_x(t)$ (Fig. 2b) that can be evaluated considering the following slab equilibrium:

$$m\ddot{u}(t) = mg_x - \mu\, mg_y + \sigma_x(t)bh \quad (1)$$

where: m is the slab mass ($m = \rho bhl$), g_x and g_y are the components of the gravity acceleration parallel and perpendicular to the slope and $\ddot{u}(t)$ is the slab acceleration in the direction parallel to the slope. The compressive normal stresses are considered to be negative.

Since snow shows viscoelastic characteristics (Mellor 1974; Salm 1975; Voytkovskiy 1977; Von Moos 2002; Von Moos *et al*.

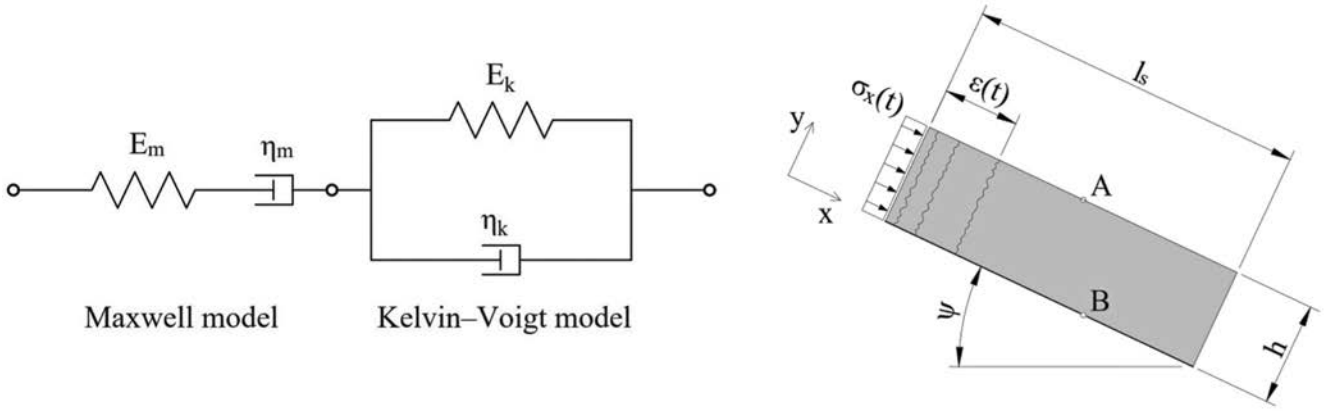

Fig. 2 – Stauchwall model: (a) schematic representation of the Burger's model; (b) detail of the stauchwall. In Fig. 2a the subscript m refers to the Maxwell dashpot η_m and spring E_m while k refers to the same elements of the Kelvin-Voigt model (η_k and E_k).

2003), Bartelt *et al*. 2012a modelled this viscoelastic behavior considering a Burger's model. This consists in a Kelvin-Voigt model in series with a Maxwell model (Fig. 2a). The stauchwall (Fig. 2b) is considered as a homogeneous prism (with density ρ, length l_s, depth h, and width b) and having no basal friction. This last assumption is true in the presence of melted water in the snowpack. It is also considered that it is possible to neglect the stauchwall stress history for $t < 0$. In addition, the displacements having direction parallel to the slope of stauchwall lower side are not allowed. Thanks to these hypotheses and considering the stauchwall as a mono-dimensional element, it is possible to find the differential equation that puts in relation the stress $\sigma_x(t)$, the strain rate $\dot{\varepsilon}(t)$ and their derivatives:

$$\ddot{\sigma}_x(t)+\left[\frac{E_m}{\eta_m}+\frac{E_m}{\eta_k}+\frac{E_k}{\eta_k}\right]\dot{\sigma}_x(t)+ \\ +\frac{E_mE_k}{\eta_m\eta_k}\sigma_x(t)=E_m\ddot{\varepsilon}(t)+\frac{E_mE_k}{\eta_k}\dot{\varepsilon}(t) \quad (2)$$

where: η_k and E_k refer, respectively, to the dashpot and the spring elements of the Kelvin-Voigt model, and η_m and E_m refer to the same elements of the Maxwell model. Note that the stauchwall self-weight is neglected in the evaluation of the stress σ_x, and this stress is assumed independent of the coordinate x.

Thanks to these assumptions, Bartelt *et al*. 2012a affirmed that the strain rate $\dot{\varepsilon}(t)$ and its derivative $\ddot{\varepsilon}(t)$ can be evaluated by knowing the slab velocity $\dot{u}(t)$ and its acceleration $\ddot{u}(t)$, as:

$$\dot{\varepsilon}(t)=-\frac{\dot{u}(t)}{2l_s} \\ \ddot{\varepsilon}(t)=-\frac{\ddot{u}(t)}{2l_s} \quad (3)$$

Therefore, by substituting Eqs. 3a and 3b in Eq. 2 the following equation is obtained:

$$\ddot{\sigma}_x(t)+\left[\frac{E_m}{\eta_m}+\frac{E_m}{\eta_k}+\frac{E_k}{\eta_k}\right]\dot{\sigma}_x(t)+ \\ +\frac{E_mE_k}{\eta_m\eta_k}\sigma_x(t)=\frac{E_m}{2l_s}\ddot{u}(t)+\frac{E_mE_k}{2l_s\eta_k}\dot{u}(t) \quad (4)$$

The system of differential equation composed by Eq. 1 and 4 represent the Stauchwall model. With the substitution of the mass definition in Eq. 1, it is possible to observe that the model is independent of both the width b and the depth h.

This system has to be numerically integrated with the following initial conditions:

$$u(0)=0, \\ \dot{u}(0)=0, \\ \sigma_x(0)=0, \\ \dot{\sigma}_x(0)=0. \quad (5)$$

reminding that $t = 0$ corresponds to the crack formation.

The stauchwall failure is attained if the strain rate $\dot{\varepsilon}(t)$ reaches the critical value $\dot{\varepsilon}_{cr}=10^{(-2)}s^{-1}$ (Bartelt *et al*. 2012a, 2012b; Feistl *et al*. 2013). In fact, the snow shows a brittle compressive failure for this strain rate which was proved thanks to triaxial tests (Scapozza and Bartelt 2003; Scapozza 2004).

Tab. I – Snow rheological parameters (Bartelt *et al*. 2012a).

ρ	E_m	η_m	E_k	η_k
kg/m^3	Pa	Pas	Pa	Pas
210	$1.0 \cdot 10^8$	$1.5 \cdot 10^9$	$2.0 \cdot 10^6$	$1.0 \cdot 10^6$
250	$1.5 \cdot 10^8$	$1.4 \cdot 10^9$	$1.5 \cdot 10^7$	$2.5 \cdot 10^6$

2. The Stauchwall Stress Model

In order to combine the original strain state stauchwall failure criterion with a stress failure one, it is necessary to evaluate the material strength and the stress state of the stauchwall after the crack opening ($t > 0$). In the Stauchwall model, the stauchwall is assumed as a viscoelastic material having no friction to the ground. Two sets of rheological parameters (Tab. 1), for two different snow densities, were adopted. These values (utilized by Bartelt *et al*. 2012a, 2012b; Feistl *et al*. 2013) were evaluated thanks to triaxial tests performed by Von Moos *et al*. 2003.

In addition, it was hypothesized that the stauchwall is isotropic (Salm 1975; Desrues *et al*. 1980; De Biagi 2009; Köchle and Schneebeli 2014) and homogeneous. The homogeneity of the snow is another aspect that can be verified when all layers of the snowpack have fully metamorphosed to wet grains thanks to high temperatures or rain (Hirashima *et al*. 2008). A last assumption was neglecting the stress history of stauchwall before the crack propagation (for $t < 0$). This assumption is anyway already considered as an initial condition for the solution of the Stauchwall model (Eq. 5).

Concerning the failure criterion added to the Stauchwall Stress Model, it is assumed that the stauchwall fails when the shear strength is reached and a Tresca failure criterion is considered.

It is assumed that the stauchwall is composed of moist snow considered having a volumetric water content θ (%). Therefore, its shear strength, which is considered uniform within the stauchwall, follows the empirical formulation of Yamanoi and Endo 2002, evaluated as a function of its dry density ρ_{dry} as:

$$\tau_{cr} = 9.40 \cdot 10^{-4} \rho_{dry}^{2.91} e^{-0.235\theta} \quad (6)$$

This formulation is valid in the range $0 \le \theta \le 8.2\%$ and for new snow, decomposed snow, and rounded grains (Yamanoi and Endo 2002; Hirashima *et al*. 2008).

To define the stauchwall stress state, the pattern in Fig. 2b is considered, where a vertical section of the stauchwall is represented. It is assumed that this section belongs to a vertical plane *x, y* and the axis *z* is perpendicular to it. The origin of *z* is at one flank of the stauchwall so that $z = b$ is the opposite flank. It can be assumed that at $z \in [0,b]$ the displacements in *z* direction are constrained by the surrounding snow. Thus, this generic stauchwall vertical plane *x, y* shows plane-strain conditions. If the vertical component of the self-weight is neglected, the stress $\sigma_y(t)$ is zero at every point belonging to the vertical line connecting two generic points *A* and *B* (Fig. 2b). Therefore, $\sigma_x(t)$ is the smallest principal stress (if $\sigma_x(t) < 0 \; \forall \; t \ge 0$) because $\sigma_y(t) = 0$ and $\sigma_z(t) = \nu(\sigma_x(t) - \sigma_y(t))$. For this reason, the maximum absolute shear stress acting in the *x, y* plane is evaluated as:

$$\tau_m(t) = \left| \frac{\sigma_x(t)}{2} \right| \quad (7)$$

and it has an inclination $\varphi = 45° - \psi$ with respect to the horizontal.

Hence, the stauchwall fails (for $t \ge 0$) when at least one of the following inequalities is true:

$$|\dot{\varepsilon}(t)| \ge |\dot{\varepsilon}_{cr}| \; OR \; |\tau_m(t)| \ge \tau_{cr} \quad (8)$$

which represents the coupled failure criterion. In fact, the inequality $|\dot{\varepsilon}(t)| \ge |\dot{\varepsilon}_{cr}(t)|$ is the criterion adopted by Bartelt *et al*. 2012a and the second inequality ($|\tau_m(t)| \ge \tau_{cr}$) is the one proposed in this work.

In the Section "Results and Discussions" some analyses are presented as well as the obtained results.

2.1. The Stauchwall Stress Model applied to a skier's fall/brake

Let's consider a slab and a stauchwall. It is possible that immediately after the crack opening the stauchwall does not fail. Therefore, the system reaches at t_1 a new equilibrium. We assume that a skier is skiing on the slab at $t \ge t_1$ in a direction parallel to the *x* axis (Fig. 2b) with a speed $v_{skier,i}$. The total mass of the skier is considered equal to $m_{skier} = 80$ kg. It is possible to suppose that at a certain time $t_1 > t_2$, the skier falls/brakes and then stops his motion ($v_{skier,f} = 0$) at a distance $d (\le l)$ along the *x* axis after a time δt_{stop}. It is supposed that this distance is completely included on the slab. Therefore, the variation of the skier's kinetic energy is:

$$\begin{aligned} \Delta K_{skier} &= \frac{1}{2} m_{skier} \delta v_{skier,i}^2 \\ &= \frac{1}{2} m_{skier} v_{skier,i}^2 \end{aligned} \quad (9)$$

where $\delta v_{skier} = v_{skier,f} - v_{skieri} = -v_{skier,i}$ is the is the skier's speed variation.

The variation of the skier's potential energy in the distance *d* is:

$$\begin{aligned} \Delta P \; v_{skier} &= m \; v_{skier} \, g d \sin\psi \\ &= m \; v_{skier} \, g_x d \end{aligned} \quad (10)$$

Thanks to the Energy Conservation Law, to stop his motion, the work that the skier must apply on the slab is:

$$W_{skier} = \Delta K_{skier} + \Delta P_{skier} = F_{stop} d \quad (11)$$

It is possible to assume that the skier applies a constant force F_{stop} on the slab in order to stop his motion. Therefore, the work applied by the skier is $W_{skier} = F_{stop} d$ and:

$$F_{stop} = m_{skier} g_x + \frac{1}{2d} m_{skier} v_{skier,i}^2 \quad (12)$$

So the skier's deceleration is constant and equal to

$$a = -\left(g_x + \frac{v_{skier,i}^2}{2d} \right)$$

and he will stop after a time:

$$\delta t_{stop} = \frac{\delta v_{skier}}{a} = \frac{2 v_{skier,i} d}{2 d g_x + v_{skier,i}^2} \quad (13)$$

For $t_2 \le t < t_3$ ($t = t_3 + \delta t_{stop}$), when the skier is decelerating, he applies a constant force to the slab. Thus, the slab equilibrium becomes:

$$\begin{aligned} m\ddot{u}(t) = m g_x - \mu m g_y + \\ + \sigma_x(t) b h + F_{stop} \end{aligned} \quad (14)$$

For $t \ge t_3$, when the skier has stopped, the force equilibrium is:

$$\begin{aligned} m_{tot}\ddot{u}(t) = m_{tot} g_x + \\ - \mu m_{tot} g_y + \sigma_x(t) b h \end{aligned} \quad (15)$$

where $m_{tot} = m + m_{skier}$.

Note that these two forces equilibrium (Eq. 14 and 15) are no longer independent of the slab width *b* and thickness *h*.

If Equation 14 is divided by the slab mass *m*, it is possible to highlight the term F_{stop}/m that represents the skier fall/brake contribution on the slab acceleration. This term should be small if the slab is very heavy. This observation is anyway examined in the Section 3.3 where the analyses results are presented.

The Equations 16a, 16b and 16c summarize the three different systems of equations that have to be used in order to evaluate the effect of a skier's fall/brake. In particular, Equation 16a represents the Stauchwall model. This Equation has to be used in the first phase when the crack propagates. Equation 16b represents the Stauchwall stress model applied to the case when on the slab a skier-braking is present (therefore called skier-braking model). In order to numerically integrate this system of equations, we assume the results of the Stauchwall model

(Eq. 16a) for $t = t_1$ (at the end of the first transient state) as initial conditions. Finally, Equation 16c is the Stauchwall-skier model. This equation is valid when the skier is on the slab immediately after he stops his motion and, for this reason, when he does not apply force to it ($t \geq t_3$). The initial conditions to solve this system (Eq. 16c) are the results of the skier-braking model (Eq. 16b) for $t = t_3$

$$for\, t < t_1 \begin{cases} \ddot{\sigma}_x(t) + \left[\frac{E_m}{\eta_m} + \frac{E_m}{\eta_k} + \frac{E_k}{\eta_k}\right]\dot{\sigma}_x(t) + \frac{E_m E_k}{\eta_m \eta_k}\sigma_x(t) = \frac{E_m}{2l_s}\ddot{u}(t) + \frac{E_m E_k}{2l_s \eta_k}\dot{u}(t) \\ m\ddot{u}(t) = mg_x - \mu mg_y + \sigma_x(t)bh \end{cases} \quad (16a)$$

$$for\, t_2 \leq t < t_3 \begin{cases} \ddot{\sigma}_x(t) + \left[\frac{E_m}{\eta_m} + \frac{E_m}{\eta_k} + \frac{E_k}{\eta_k}\right]\dot{\sigma}_x(t) + \frac{E_m E_k}{\eta_m \eta_k}\sigma_x(t) = \frac{E_m}{2l_s}\ddot{u}(t) + \frac{E_m E_k}{2l_s \eta_k}\dot{u}(t) \\ m\ddot{u}(t) = mg_x - \mu mg_y + \sigma_x(t)bh + F_{stop} \end{cases} \quad (16b)$$

$$for\, t \geq t_3 \begin{cases} \ddot{\sigma}_x(t) + \left[\frac{E_m}{\eta_m} + \frac{E_m}{\eta_k} + \frac{E_k}{\eta_k}\right]\dot{\sigma}_x(t) + \frac{E_m E_k}{\eta_m \eta_k}\sigma_x(t) = \frac{E_m}{2l_s}\ddot{u}(t) + \frac{E_m E_k}{2l_s \eta_k}\dot{u}(t) \\ m_{tot}\ddot{u}(t) = m_{tot} g_x - \mu m_{tot} g_y + \sigma_x(t)bh \end{cases} \quad (16c)$$

3. Results & Discussions

The results and discussions of the performed numerical analyses are presented in this Section. At the beginning, attention is given to the results of analyses carried out using the Stauchwall model. Subsequently, the results and comments on the delayed releases and the skier's triggering are reported. Finally, the results of the sensitivity analyses are shown and some observations for the control and prevention of these avalanches are given.

3.1. Stauchwall model analysis

The results of the analyses carried out using the Stauchwall model are presented in this Section. In particular, investigations on the failure criteria and stauchwall length are performed.

Stauchwalls are not so well defined in real cases and they may be partially destroyed after the avalanche release. Thus, the stauchwall length is difficult to be measured/estimated. In Figure 3 the results of six analyses meant to study the influence of these length estimations are presented. In these two graphs the shear strength τ_{cr} (θ = 0) and the critical strain rate $\dot{\varepsilon}_{cr}$ are also plotted. The analyses were carried out considering a fixed total length $l + l_s$ = 30m, ψ = 35°, μ = 0.45 and three stauchwall lengths l_s = 1,2 and 4 m. For what regards the first three analyses, the assumed density (with the corresponding rheological parameters) is ρ = 250 kg/m^3 and results are reported in Figure 3a. A density ρ = 210 kg/m^3 (with the related rheological parameters) is considered for the other three analyses and the results are displayed in Figure 3b.

From Figure 3 it is possible to notice that the stauchwall length estimation has a much larger effect on the maximum strain rate than the maximum shear stress. Assume as a reference the results obtained using a stauchwall length of 2 m and a density ρ = 250 kg/m^3. If this length is halved the maximum strain rate increases by 34 % (23 % for ρ = 210 kg/m^3) while the maximum shear stress increments by 12 % (11 % for ρ = 210 kg/m^3). Similarly, doubling the stauchwall length (l_s = 4 m) implies a 26 % reduction of the maximum strain rate (17 % for ρ = 210 kg/m^3) while the maximum shear stress decreases by 13 % (7 % for ρ = 210 kg/m^3). Since the stauchwall length has to be supposed and the stauchwall stress is less sensitive to this hypothesis, the stress criterion should help to understand if the stauchwall fails. This fact can be verified by paying more attention to Figure 3a. It is possible to notice that the snowpack under study fails, by reaching only the critical strain, only if a stauchwall length of l_s = 1 m is assumed. In parallel, if the shear strength is taken as a failure criterion, the assumption of the stauchwall length is less important since for both l_s = 1 and 2 m the stauchwall will fail.

It is interesting to highlight that it is possible to determine if the stauchwall failure is due to the stress criterion or to the strain rate criterion. To do this it is necessary to evidence that the curves obtained in Figure 3 have to be read in an anticlockwise direction starting from the axes origin. As example, let's consider the results of the analysis performed considering l_s = 2 m and ρ = 210 kg/m^3 (Fig. 3b). It is possible to affirm that in this case the avalanche is released because the critical strain rate is attained while the stauchwall stress never reaches the material strength. As a matter of fact, proceeding on the curve starting from the axes origin, the critical strain rate is the

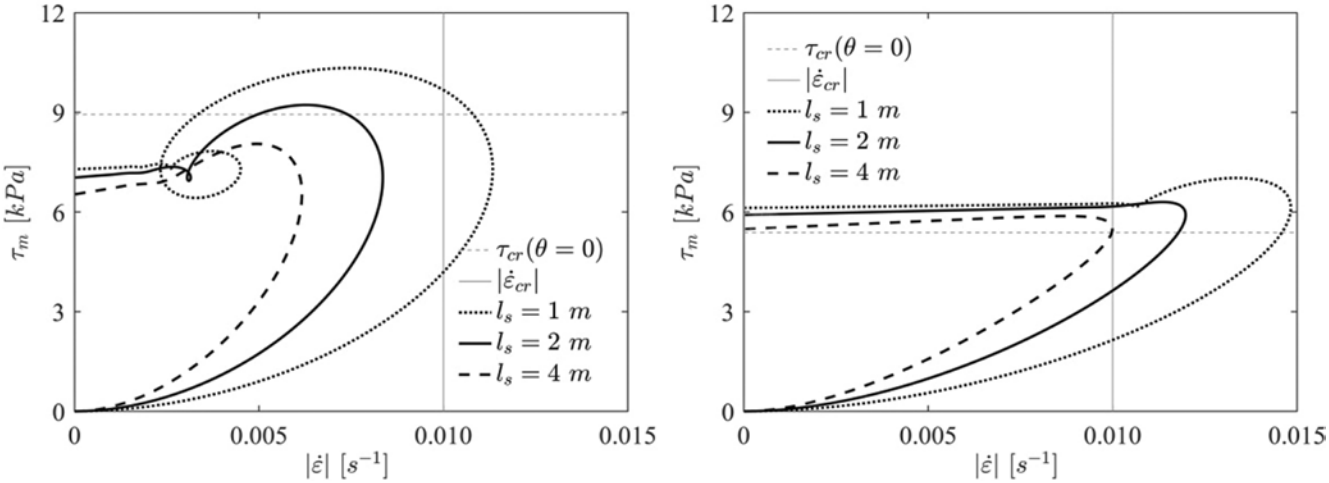

Fig. 3 – The plots show the results considering a fixed total length $l + l_s$ = 30 m, three stauchwall lengths l_s = 1,2 and 4 m, ψ = 35°, μ = 0.45. Figure 3a shows the results of the analyses carried out considering a density ρ = 250 kg/m^3. The results of the analyses carried out assuming ρ = 210 kg/m^3 are displayed in Figure 3b. In the plots the shear strength (τ_{cr} (θ = 0)) and the absolute value of the critical strain rate $\dot{\varepsilon}_{cr}$ are represented.

first line intersected by the curve. This means that the remaining part of the curve is just theoretical since the avalanche is triggered as soon as the critical strain is reached. Therefore, it is possible to distinguish in between failures.

Another important fact can be pointed out looking at the results obtained for ρ = 210 kg/m^3 and l_s = 4 m (Fig. 3b). In this case it is difficult to be sure if the avalanche is released only by looking at the strain rate criterion. However, the stauchwall failure is clear considering the stress criterion. This fact highlights the importance of coupling these two criteria.

The results of analyses performed considering a snow density ρ = 250 kg/m^3 (with the related rheological parameters), a stauchwall length l_s = 2 m and varying the slope inclination and the slab length are summarized in Figure 4. The target of these analyses is to calculate the frictions for which the avalanche is triggered and to define if the release is caused because the critical strain rate is attained (solid color) or if the shear strength is reached (top bar prisms with transparency). It can be observed that the critical strain rate is exceeded when relatively small friction values are considered. The cases of avalanches due to the fact that shear strength is attained correspond to small intervals of friction values only. From Figure 4 it is interesting to observe that the stress criterion is stricter. In detail, if the strain rate criterion is the only one adopted, it is possible to underestimate the minimum friction value necessary to avoid a glide avalanche because with this value the material strength is exceeded and the avalanche is triggered.

3.2. Delayed releases

Thanks to the stress failure criterion it is possible to examine delayed releases. Let's consider the Stauchwall model (Eq. 16a) and let's suppose that in the transient state

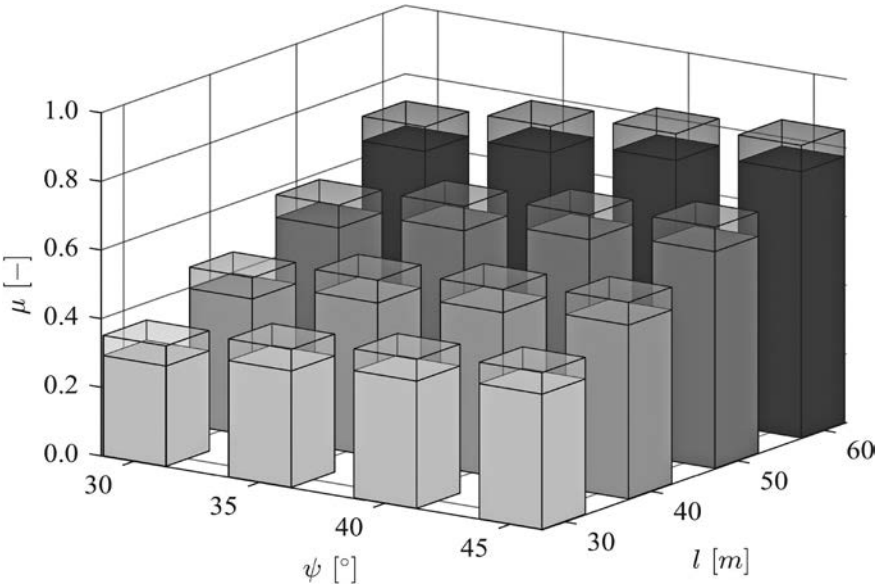

Fig. 4 – The image displays a three-dimensional plot showing the friction values necessary to trigger the avalanches considering different slope inclinations and slab lengths. This graph has been computed considering a density ρ = 250 kg/m^3 (with the related rheological parameters of Tab. 1), and a stauchwall length l_s = 2 m. The solid color of the bars represents the frictions for which the critical strain rate is attained while the top bar prisms, with transparency, represent the friction values for which the shear strength (τ_{cr} (θ = 0)) is attained.

the stauchwall did not fail. It is possible to consider the curve obtained considering l_s = 4 m in Figure 3a as example. In this case, for a certain time $t_1 > 0$ coincident with the end of the transient state, a new equilibrium exists. This time t_1 can be defined as the time in which the slab acceleration becomes constant and equal to zero. Therefore, the stress becomes constant and equal to:

$$\sigma_x(t \geq t_1) = \rho g l(\mu\cos\psi - \sin\psi) \quad (17)$$

and the strain rate becomes $\dot{\varepsilon}(t \geq t_1) = \sigma_x(t \geq t_1) / \eta_m$ (therefore $\ddot{\varepsilon}(t \geq t_1) = 0$). Since both the strain rate and the shear stress are constant and considering that the failure is not attained for $t > t_1$, the avalanche can be triggered only by two factors, an equilibrium perturbation or a loss of strength.

A perturbation of the slab-stauchwall equilibrium can be caused, as an example, by an increasing presence of melted water at the snow-soil interface which reduces the basal friction μ. It is possible to suppose that this variation (which starts at the generic time $t_2 \geq t_1$) is very slow so that the strain acceleration is almost zero while the stress inside of the stauchwall increases (Eq. 17). For this reason, it is not possible to attain the critical strain rate. However, the stauchwall can fail because the shear strength is attained (e.g. dashed line in Fig. 5).

The second possible cause of a delayed release is a reduction of the material strength. To take into account this strength variation, it is possible to suppose that at $t = t_2$ the snow is on the slope and that its humidity starts to increase (due, as example, to solar irradiation or to rain). This water content raise produces a reduction of the snow shear strength (Eq. 6). Thus, the stauchwall stress can arrive at the material strength and, as consequence, the avalanche is triggered (e.g., dotted line in Fig. 5).

An even more realistic situation can be the combination of both the mechanisms presented before (e.g., solid line in Fig. 5). In fact, water due to metamorphism/rain may act on both the basal friction and the shear strength.

3.3. Skier's triggering

The analysis of a skier that stops over a slab is presented in Figure 6 (Eq. 16a, b and c). This specific case represents a perturbation of the slab equilibrium. Therefore, if the avalanche is triggered by the skier, it is possible to consider it as a delayed release. With the notation previously introduced, the parameters assumed in the analysis are b = 10 m, t = 0.5 m, l_s = 2 m, l = 20 m, ψ = 35°, ρ = 250 kg/m^3 (and the related rheological parameters of Tab. 1), v_{skier} = 13.9 m/s and d = 10 m. The results are presented in Figure 6. It is possible to note that the effects of the skier's fall/brake are quite limited in terms of shear stress while they are more marked in terms of strain rate. The critical values are not attained in both cases. It has to be underlined that no changes in basal friction and shear strength were considered during the analysis. Moreover, it is important to point out that the results are dependent on the slab mass.

In fact, according to the model introduced in Sub-section 2.1, the outcomes of some analyses underlined the fact that a fall/brake of a skier has noticeable effects only in very light slabs. In this case, the critical strain rate may be attained while the increase of shear stress is relatively small. As example, the critical strain rate in the stauchwall is attained due to the skier's fall/brake considering the following parameters b = 0 m, t = 0.3 m, l_s = 2 m, l = 10 m, ψ = 35°, ρ = 250, ψ = 35°, ρ = 250 kg/m^3 (and the related rheological parameters of Tab. 1), v_{skier} = 13.9 m/s and d = 5 m. However, if the snowpack thickness is increased by

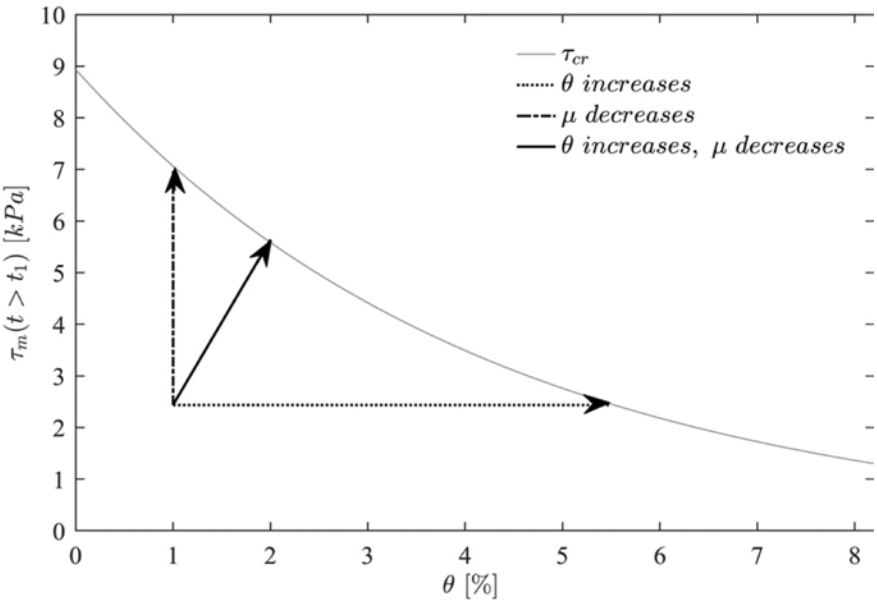

Fig. 5 – The image displays a graph in which the snow resistance domain (for a fixed density) is defined as the area under the grey line which represents the shear strength as a function of the volumetric water content. It is then considered a stauchwall that does not fail after the glide crack propagation (considering θ = 1%, l = 20 m, l_s = 2 m, ρ = 250 kg/m^3, ψ = 30°, and μ = 0.50 and the related rheological parameters of Tab. 1). The generic point of coordinates θ = 1%, $\tau_m(t > t_1)$ = 2.5 kPa represents the stauchwall status at $t = t_1$ and it is coincident with the point from which the three straight lines generate. The dotted line represents the evolution of the stauchwall status due to the increase of water content, the dashed line represents a basal friction decrease and the solid line is a combination of both mechanisms.

just 5 cm, the maximum stauchwall strain rate results below to the critical value. Similarly, if the distance *d* is increased by one meter, the critical strain value is not reached. In literature (Feistl *et al*. 2014; van Herwijnen and Simenhois 2012) glide avalanche having short slabs and thin snow covers are recorded even if, unfortunately, slabs widths are not reported. However, these cases represent a relatively small amount of the field observations. Therefore, it seems plausible (even if not very probable) that, after a crack propagation, the snow remains on the slope and that a skier can trigger the glide avalanche.

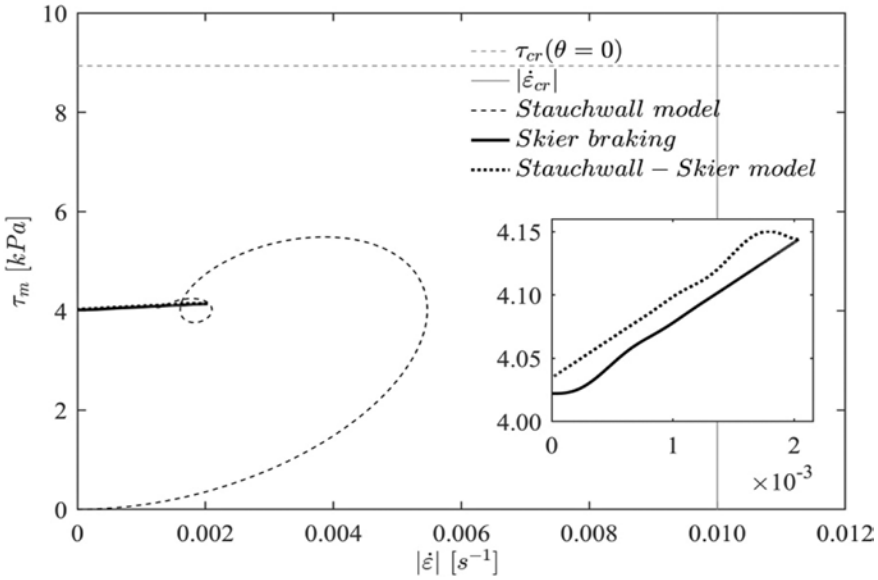

Fig. 6 – The image shows an analysis performed considering at first the results of the Stauchwall model then the effect of the skier's braking and finally the transient of the new system. The shear strength and the critical strain rate are also plotted in the graph.

3.4. Sensitivity analysis

An investigation of the model sensitivity has been carried out. This investigation is implemented using the Stauchwall model (Eq. 16a) without considering the failure criteria. In particular, a base analysis is performed considering the following parameters: b = 30 m, t = 0.5 m, l_s = 2 m, l = 30 m, ψ = 35°, μ = 0.35, ρ = 250 kg/m^3 and the related rheological parameters (Tab. 1). Subsequently, one by one, all the parameters are varied by ±5% in order to understand the role played by them in the model results. It has to be underlined that the results of the Stauchwall model are independent of the slab width b and thickness t.

The results of this sensitivity analysis are summarized in Figure 7. This plot was created in order to point out the important role played by the basal friction μ and by the slope inclination ψ. In fact, these two parameters are the ones that most affect the model results. The variation of all the other parameters creates a relatively small change in the results. This is evidenced with a grey area in Figure 7.

The results show that the evaluation of both the basal friction and the slope inclination is crucial in order to have a reliable model. Of course, it is much simpler to measure a relatively precise value of slope inclination rather than assess the basal friction, that is of more uncertain and delicate determination. This value depends on many slope characteristics like type of surface, surface roughness, type of vegetation, vegetation length, presence of water, etc.

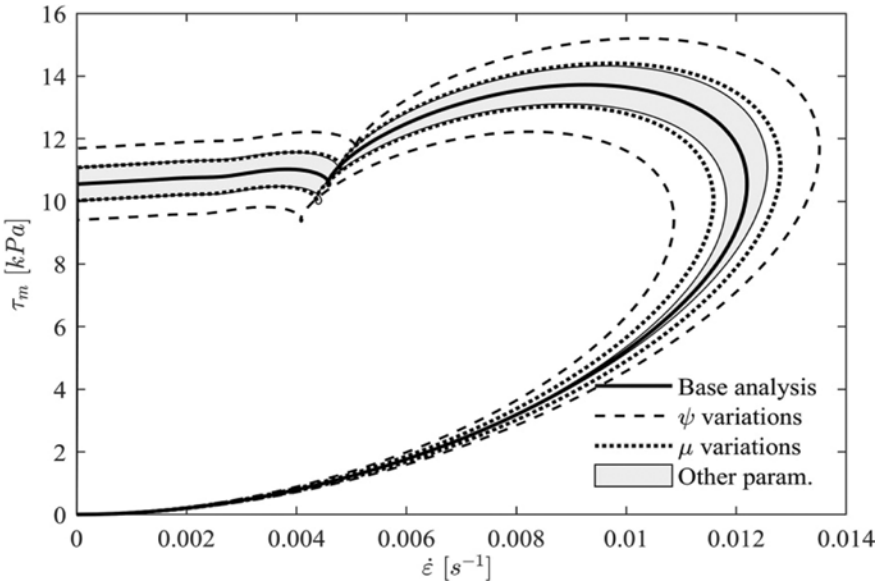

Fig. 7 – The image shows the results of the sensitivity analysis. The continuous thick line represents the base analysis, the dashed curves are the variations of the slope inclination ψ. The variations of the basal friction μ are plotted with a dotted curve and the grey area encloses the variations of all the other parameters.

3.5. Prevention & control

In this Subsection, some ideas regarding the prevention and control of glide avalanches are made thanks to a general view of the results reported in the previously Subsections.

It is possible to start by recalling the two examined mechanisms as possible delayed release causes be-

cause it is interesting to consider them in order to artificially trigger glide avalanches. Water could be used in order to reduce the basal friction by pouring it in the crack using a helicopter. A second possibility is the reduction of the material strength by watering the stauchwall. However, this method can imply a large quantity of water. In fact, 10 kg of water are necessary in order to produce a 1 % increase in the volumetric water content per m^3 of snow. A third solution consists in coupling these two methods. At first, it is possible to act on the stauchwall to enable the water to decrease the shear strength. Water can be poured into the glide crack at the second transit of the aircraft. However, these methods (even if they are coupled) do not guarantee an immediate (or predictable with a good certainty) release which is not perfect in accordance with the principles of artificial triggering. As a subsequent action, water can be used to strike the slab. This operation can act on the slab equilibrium in a way like the skier's fall/break. Unfortunately, it is not simple to compute the effect of this strike. However, although large helicopters having large buckets can carry up to ~2-4 m^3 of water, the effect of the strike may be negligible if the targets are very heavy slabs. Moreover, the Stauchwall model considers rigid slabs while the real snow could absorb part of the impact energy.

The important role that the basal friction plays in the Stauchwall model results was underlined in the sensitivity analysis. This effect can be interpreted in another way: small increases of this characteristic reduce noticeably the strain rate and shear stress inside the stauchwall. This fact can be used for avalanche prevention. On slopes where frequent glide avalanches occur, short furrows (perpendicular to the maximum slope inclination) may be created. Otherwise, as less impacting measure, the grass can be shortened before the winter (cutting it or using animals which graze it) or shrubs can be implanted. Feistl *et al*. 2014 pointed out as these two slope characteristics (short grass and shrubs presence) are related to glide avalanches having longer slab and that occurred on steeper slopes. Another way to interpret this observation points out that shorter grass and shrubs prevent glide avalanches in cases of short slabs and mild slopes.

4. Conclusions

The present work focuses on the study of glide avalanches. In particular, analyses were performed using the Stauchwall model for which a stress failure criterion was coupled with the criterion adopted in previous works. The numerical results show that glide avalanches may be triggered because the snow shear strength is attained while the critical strain rate is not. It was also proved that the utilization of just the critical strain rate as a failure criterion may lead to underestimation of safe basal friction values.

In glide avalanches, it is difficult to define/measure the stauchwall length which is an important parameter in the Stauchwall model. The present work shows that the stauchwall length estimation has much larger effects on the maximum strain rate rather than the maximum shear stress. Therefore, the Stauchwall Stress model could be an interesting option.

An important characteristic of these avalanches is that they may be not triggered immediately after the crack propagation but after several hours or days. The Stauchwall stress model has been used in order to make some considerations regarding these delayed releases thanks to the adopted new failure criterion. Hence, it was proved how an increase of the stauchwall water content or/and a reduction of the basal friction can lead to the avalanche release.

The proposed model has been also expanded to consider the skier's fall/brake over the slab. The results show as this effect may trigger a glide avalanche in the case of very light slabs.

The sensitivity analysis has highlighted how small variations in the slope angle and in the basal friction lead to quite noticeable variations in Stauchwall stress model results.

Finally, some considerations regarding possible methodologies meant to prevent and/or control glide avalanches are presented. A possible artificial trigger methodology has been outlined. It has been then pointed out how the stauchwall stress model sensitivity to the basal friction could be used as a glide avalanche prevention method.

Further studies may focus their attention on many influencing aspects. Rheological parameters of different snow types may be important in order to apply more effectively the stauchwall model. Studies meant to determine the stauchwall length can be crucial since this length plays a very important role. Moreover, model refinements may give more realistic results. It can be interesting, for example, to consider the effect of the basal friction under the stauchwall or no longer consider the stauchwall as a lumped element and model it as a viscoelastic continuum.

References

Ancey, C., Bain, V., (2015). Dynamics of glide avalanches and snow gliding. Reviews of Geophysics 53 (3): 745-784.

Baggi, S., Schweizer, J., (2009). Characteristics of wet-snow avalanche activity: 20 years of observations

from a high alpine valley (Dischma, Switzerland). Natural Hazards 50 (1): 97-108.

Bartelt, P., Feistl, T., Bühler, Y., and Buser, O., 2012a. Overcoming the stauchwall: Viscoelastic stress redistribution and the start of full-depth gliding snow avalanches. Geophysical research letters 39 (16).

Bartelt, P., Pielmeier, C., Margreth S., Harvey, S., Stucki, T., (2012b). The underestimated role of the stauchwall in full-depth avalanche release, in Proceedings of the International Snow Science Workshop, 127-133.

Conway, H., Raymond, C.F., (1993). Snow stability during rain. Journal of Glaciology 39 (133): 635-642.

De Biagi, V., (2009). Opening angle of loose-snow avalanches. Geoingegneria Ambientale e Mineraria 50 (1): 97-108.

der Gand, H.I., Zupančič, M., (1965). Snow gliding and avalanches 9:201-213. IAHS-Publ.

Desrues, J., Darve, F., Flavigny, E., Navarre, J.P., Taillefer, A., (1980). An Incremental Formulation of Constitutive Equations for Deposited Snow. Journal of Glaciology 25 (92): 289-307. doi:10.3189/S0022143000010509

Feistl, T., Bebi, P., Bartelt, P., (2013). The role of slope angle, ground roughness and stauchwall strength in the formation of glide-snow avalanches in forest gaps, in Proceedings of the 2013 International Snow Science Workshop, Grenoble, France, 760-765.

Feistl, T., Bebi, P., Dreier, L., Hanewinkel, M., Bartelt, P., (2014). Quantification of basal friction for technical and silvicultural glide-snow avalanche mitigation measures. Natural Hazards and Earth System Sciences 14 (11): 2921.

Hirashima, H., Nishimura, K., Yamaguchi, S., Sato, A., Lehning, M., (2008). Avalanche forecasting in a heavy snowfall area using the snowpack model. International Snow Science Workshop (ISSW) 2006, Cold Regions Science and Technology 51 (2): 191-203. ISSN: 0165-232X. doi:https://doi.org/10.1016/j.coldregions.2007.05.013. http://www.sciencedirect.com/science/article/pii/S0165232X07001279

Höller, P., (2014). Snow gliding and glide avalanches: a review. Natural hazards 71 (3): 1259-1288.

Köchle, B., Schneebeli, M., (2014). Three-dimensional microstructure and numerical calculation of elastic properties of alpine snow with a focus on weak layers. Journal of Glaciology 60 (222): 705-713. doi:10.3189/2014JoG13J220

Lackinger, B., (1987). Stability and fracture of the snow pack for glide avalanches. International Association of Hydrological Sciences Publication 162: 229-240.

McClung, D.M., (1981). A physical theory of snow gliding. Canadian Geotechnical Journal 18 (1): 86-94.

McClung, D., Clarke, G.K.C., (1987). The effects of free water on snow gliding. Journal of Geophysical Research: Solid Earth 92 (B7): 6301-6309.

McClung, D., Schaerer, P.A., (1993). The avalanche handbook. Mountaineers.

Mellor, M., (1974). A review of basic snow mechanics. US Army Cold Regions Research / Engineering Laboratory.

Peitzsch, E.H., Hendrikx, J., Fagre, D.B., Reardon, B., (2012). Examining spring wet slab and glide avalanche occurrence along the Going-to-the-Sun Road corridor, Glacier National Park, Montana, USA. Cold Regions Science and Technology 78:73-81. ISSN: 0165-232X. doi:https://doi.org/10.1016/j.coldregions.2012.01.012. http://www.sciencedirect.com/science/article/pii/S0165232X12000250

Salm, B., (1975). A constitutive equation for creeping snow. International Association of Hydrological Sciences Publication 114: 222-235.

Scapozza, C., Bartelt, P., (2003). Triaxial tests on snow at low strain rate. Part II. Constitutive behaviour. Journal of Glaciology 49 (164): 91-101.

Scapozza, C., (2004). Entwicklung eines dichte-und temperaturabhängigen Stoffgesetzes zur Beschreibung des visko-elastischen Verhaltens von Schnee. vdf Hochschulverlag AG. Vol. 15357.

Simenhois, R., Birkeland, K., (2010). Meteorological and environmental observations from three glide avalanche cycles and the resulting hazard management technique, in International Snow Science Workshop ISSW, Lake Tahoe CA, USA, 846-853.

Stimberis, J., Rubin, C.M., (2011). Glide avalanche response to an extreme rain-on-snow event, Snoqualmie Pass, Washington, USA. Journal of Glaciology 57 (203): 468-474.

van Herwijnen, A., Simenhois, R., (2012). Monitoring glide avalanches using time-lapse photography, in International Snow Science Workshop ISSW, 899-903.

Von Moos, M., (2002). Untersuchungenüber das visko-elastische Verhalten von Schnee auf der Grundlage von triaxialen Kriechversuchen. vdf Hochschulverlag AG. Vol. 13725.

Von Moos, M., Bartelt, P. Zweidler, A., Bleiker, E., (2003). Triaxial tests on snow at low strain rate. Part I. Experimental device. Journal of Glaciology 49 (164): 81-90.

Voytkovskiy, K.F., (1977). Mekhanicheskiye svoystva snega. CE Bartelt (trans.), Moscow, Nauka. Sibirskoye Otdeleniye. Institut Merzlotovedeniya.

Yamanoi, K., and Endo, Y., (2002). Dependence of shear strength of snow cover on density and water content. Journal of the Japanese Society of Snow and Ice 64 (4): 443-451.

Declaration of interest

The authors declare no conflict of interest, financial or otherwise.